Analyzing the H_0 tension in $F(R)$ gravity models

Sergei D. Odintsov,[1,2,*] Diego Sáez-Chillón Gómez,[3,†] and German S. Sharov[4,5,‡]

[1]*Institut de Ciències de l'Espai, ICE/CSIC-IEEC, Campus UAB,*
Carrer de Can Magrans s/n, 08193 Bellaterra (Barcelona), Spain
[2]*Institució Catalana de Recerca i Estudis Avançats (ICREA),*
Passeig Luis Companys, 23, 08010 Barcelona, Spain
[3]*Department of Theoretical, Atomic and Optical Physics, Campus Miguel Delibes,*
University of Valladolid UVA, Paseo Belén, 7, 47011 Valladolid, Spain
[4]*Tver state university, Sadovyj per. 35, 170002 Tver, Russia*
[5]*International Laboratory for Theoretical Cosmology,*
Tomsk State University of Control Systems and Radioelectronics (TUSUR), 634050 Tomsk, Russia

The Hubble constant tension problem is analysed in the framework of a class of modified gravity, the so-called $F(R)$ gravity. To do so, we explore two models: an exponential and a power-law $F(R)$ gravities, which includes an early dark energy (EDE) term in the latter. These models can describe both an early time inflationary epoch and the late time accelerating expansion of the universe. We confront both models with recent observational data including the Pantheon Type Ia supernovae sample, the latest measurements of the Hubble parameter $H(z)$ from differential ages of galaxies (cosmic chronometers) and separately from baryon acoustic oscillations. Standard rulers data set from the Cosmic Microwave Background radiation are also included in our analysis. The estimations of the Hubble constant appear to be essentially depending on the set of observational data and vary in the range from 68 to 70.3 km/(s·Mpc). The fits of the other free parameters of the models are also obtained, revealing interesting consequences.

I. INTRODUCTION

Among current problems in modern cosmology, the tension among estimations of the Hubble constant H_0 is one of the most striking and irritating for researchers. Over the last years such discrepancies among H_0 measurements have been revealed through two different methods: by the Planck collaboration after collecting and analyzing data from the cosmic microwave background radiation (CMB) over the last 7 years [1–3], which provides an estimation of $H_0 = 67.4 \pm 0.5$ km s^{-1}Mpc^{-1} (Planck18), and on the other hand by the SH0ES group of Hubble Space Telescope (HST) [4, 5] with the last estimate given by $H_0 = 74.03 \pm 1.42$ km s^{-1}Mpc^{-1} (SH0ES19). The HST method includes measurements of the local distance ladder by combining photometry from Cepheids (and their period luminosity relation) with other local distance anchors, Milky Way parallaxes and calibration distances to Cepheids in the nearest galaxies which are hosts of Type Ia Supernovae (SNe Ia). In particular, the above estimation for the Hubble constant by the HST group includes observations of 70 Cepheids in the Large Magellanic Cloud [5].

Currently the mismatch among H_0 estimations by Planck [3] and HST [5] collaborations exceeds 4σ, as this tension has grown over the last years, as shown in Table I. This problem may be dealt as the discrepancy between observations at early and late cosmological time of our Universe [6], since HST group works with late time data while Planck collaboration combines observations from redshifts in a wide range $0 < z < 1100$ and uses the standard ΛCDM model as fiducial model, but the issue may be approached through a theoretical way. For the former, some researchers have suggested some different ways for solving the H_0 tension problem. Several groups have analysed the estimations of H_0 by using several approaches independent of the Cepheid distance scale and CMB anisotropies (for a review see [6, 7]). Among these methods with new observational results for H_0, the following approaches may be highlighted: the tip of the red giant branch (TRGB) method used by the Carnegie-Chicago Hubble Program (CCHP) [8, 9], lensing objects with strong time delays between multiple images (H0LiCOW project and others) [10–12], CMB-lensing data [13], maser (megamaser) hosting galaxies [14], oxygen-rich variable stars (Miras) [15]. Some other researchers tried to explain the tension by assuming that Planck or HST measurements might suffer from systematic

*Electronic address: odintsov@ice.csic.es
†Electronic address: diego.saez@uva.es
‡Electronic address: sharov.gs@tversu.ru

errors [16], but these analysis did not led to convincing solutions of the problem.

As shown in Table I, one can note that most of H_0 estimations lie on the range among Planck18 and SH0ES19 values, while the local (late-time) H_0 measurements are close to the SH0ES19 value, exceed the early-Universe estimations. Only the CCHP estimation obtained by TRGB method violates the latter tendency, which have led to some discussions [6, 9]. By comparing these facts, many cosmologists over the recent years have considered the H_0 tension as a hint for new physics beyond the standard ΛCDM model with different phenomena in early and/or late times of the universe evolution [17]–[23] (see also the extended list of literature in Ref. [7]). These analysis suggest several ways for solving the problem, which can be generally summarized as a mechanism that shifts the effective H_0 value from early to late time Universe under different factors. The best fit H_0 appears to be essentially depending on the mentioned factors. Following this idea, some scenarios have been studied:

- Dark energy models with a varying equation of state (EoS), via a varying EoS parameter w or via the dark energy density ρ_{DE} [17].

- Scenarios with an early dark energy (EDE) component, reproduced in different frameworks (scalar fields, axions), which becomes important before the epoch of matter-radiation equality $z \simeq 3000$ and then decays after faster than radiation [18].

- Models with evolving or decaying dark matter into dark radiation or other species [19].

- Interacting dark energy and dark matter models [20].

- Models with extra relativistic species that modifies the effective number N_{eff} at the recombination era [21].

- Modified gravity models that emerge at an intermediate epoch, as scalar-tensor theories, $F(R)$ gravity, $F(T)$ and others [22–24].

Project	Year	H_0 (km s^{-1}Mpc^{-1})	Method	Refs
Planck	2018	67.4 ± 0.5	CMB power spectra+lensing	[3]
SH0ES (HST)	2019	74.03 ± 1.42	Cepheid distance ladder	[5]
CCHP	2020	$69.6 \pm 0.8 \pm 1.7$	TRGB	[9]
H0LiCOW	2019	$73.3^{+1.7}_{-1.8}$	6 strong lenses & ΛCDM	[10]
-	2020	$75.3^{+3.0}_{-2.9}$	7 strong lenses + SNe Ia	[11]
-	2020	$71.8^{+3.8}_{-3.3}$	8 strong lenses & ΛCDM	[12]
-	2020	73.5 ± 5.3	CMB lensing + SNe Ia	[13]
Megamaser	2020	73.9 ± 3.0	6 maser galaxies	[14]
HST	2019	72.7 ± 4.6	6 Miras in SN Ia host galaxy	[15]

TABLE I: Recent estimations of the Hubble constant H_0

In this sense, modified gravities have been widely studied in the literature in the framework of cosmology (for a review see [25]). Particularly, $F(R)$ gravity is very well known by the scientific community, with an extensive literature where many aspects of the theory have been analysed. This modification of GR assumes a generic function of the Ricci scalar for the gravitational action instead of the linear term of the Hilbert-Einstein action. Such modification leads to interesting properties and a rich phenomenology that can solve some of the most important problems in cosmology, as the origin of dark energy. In this sense, $F(R)$ gravity can reproduce well the late-time acceleration with no need of additional fields and alleviate the cosmological constant problem by compensating the large value for the vacuum energy density predicted by quantum field theories (see [26–31]). In addition, the same type of modifications of GR have been studied in the framework of inflation where as in the case of dark energy, $F(R)$ gravities can lead to successful scenarios that fit perfectly well the constraints on the spectral index of perturbations as given by the analysis of the CMB ([32]). With this in mind, models that unify the dark energy epoch and the inflationary paradigm through the corrections introduced in the gravitational action have been proposed with a great success [33–40]. In addition, some $F(R)$ gravity models that reproduce late-time acceleration can also recover GR at local scales where this one is very well tested, leading to the so-called viable $F(R)$ gravity models [28, 29]. Hence, $F(R)$ gravity is particularly of great interest in cosmology.

Hence, supported on the the great knowledge of $F(R)$ gravity and its success on trying to solve some of the most important problems in cosmology, the possibility of alleviating the H_0 tension problem in this framework may be promising, despite has not been studied yet exhaustively. Although some efforts are being done, as the analysis to solve this tension by viable $F(R)$ models, and particularly through the Hu-Sawicki $F(R)$ model [28] in Ref. [23],

where concluded that the Hu-Sawicki gravity cannot reduce the H_0 tension. In the present paper, we analyse two $F(R)$ models and the possibility of alleviating the H_0 tension. We confront the models with observational data and estimate the Hubble constant H_0 and other model parameters by using approaches developed in some previous papers [34, 35, 41–44]. Here we include in our analysis the following observations: the Type Ia supernovae data (SNe Ia) from the Pantheon sample survey [45], data connected with cosmic microwave background radiation (CMB) and extracted from Planck 2018 observations [3, 46], and estimations of the Hubble parameter $H(z)$ for different redshifts z from two different sources: (a) measured from differential ages of galaxies (in other words, from cosmic chronometers, these 31 data points are analyzed separately) and (b) $H(z)$ obtained as observable effect of baryon acoustic oscillations (BAO). We obtain the best fit parameters and compare to the ones from ΛCDM.

The paper is organized as follows. In section II, we introduce $F(R)$ gravity and the two models we analyse along the paper. Section III is devoted to SNe Ia, $H(z)$ and CMB observational data. In section IV we analyze the results, estimations for the Hubble constant H_0 and other model parameters. Finally, section V gathers the conclusions of the paper.

II. $F(R)$ GRAVITY MODELS

We can start by reviewing the basics of what is called $F(R)$ gravity, a generalization of the Einstein-Hilbert action that assumes a more complex Lagrangian in terms of the Ricci scalar R:

$$S = \frac{1}{2\kappa^2} \int d^4x \sqrt{-g}\, F(R) + S^{\text{matter}} . \tag{1}$$

Here $\kappa^2 = 8\pi G$ and S^{matter} is the matter action. In the present paper, we are interested in analyzing the H_0 tension problem in the framework of $F(R)$ gravity with the following general form for the action [37]:

$$F(R) = R + F_{\text{inf}} + F_{\text{EDE}} + F_{\text{DE}} . \tag{2}$$

The first term here is the Einstein-Hilbert action, F_{inf} is assumed to describe the early-time inflation [37–39] becoming negligible at late times $z < 3000$ (only this epoch is visible in our observational data), whereas F_{DE} plays the role of dark energy, dominating at late times, and is the object under study in this paper. Finally, we have added an extra term, F_{EDE}, that behaves as an early dark energy (EDE) term, i.e. mimics an effective cosmological constant at intermediate times but then dilutes along the expansion, helping to suppress some inadequate behaviors during the intermediate phases between the matter-radiation equality and recombination [18]. The general field equations for $F(R)$ gravity are obtained by varying the action (1) with respect to the metric $g_{\mu\nu}$, leading to:

$$F_R R_{\mu\nu} - \frac{F}{2} g_{\mu\nu} + \left(g_{\mu\nu} g^{\alpha\beta} \nabla_\alpha \nabla_\beta - \nabla_\mu \nabla_\nu\right) F_R = \kappa^2 T_{\mu\nu} ,$$

where $R_{\mu\nu}$ and $T_{\mu\nu}$ are the Ricci and energy-momentum tensors respectively. By assuming a spatially-flat Friedman-Lemaître-Robertson-Walker (FLRW) space-time

$$ds^2 = -dt^2 + a^2(t)\, d\mathbf{x}^2$$

with the scale factor $a(t)$, the FLRW equations in $F(R)$ gravity are obtained:

$$\frac{dH}{d\log a} = \frac{R}{6H} - 2H,$$

$$\frac{dR}{d\log a} = \frac{1}{F_{RR}} \left(\frac{\kappa^2 \rho}{3H^2} - F_R + \frac{RF_R - F}{6H^2}\right), \tag{3}$$

$$\frac{d\rho}{d\log a} = -3(\rho + p). \tag{4}$$

The continuity equation (4) can be easily solved for dust matter ρ_m and radiation ρ_r and yields

$$\rho = \rho_m^0 a^{-3} + \rho_r^0 a^{-4} = \rho_m^0 (a^{-3} + X_r a^{-4}) . \tag{5}$$

Here $a = 1$, ρ_m^0 and ρ_r^0 are the present time values of the scale factor and the matter densities, while we assume the following estimation for the ratio among densities as provided by Planck [1]:

$$X_r = \frac{\rho_r^0}{\rho_m^0} = 2.9656 \cdot 10^{-4} . \tag{6}$$

The aim of this paper is to explore and compare two clases of $F(R)$ models of the type described by (2). In both cases, we neglect the inflationary term given by F_{inf} and assume some initial conditions that mimic ΛCDM model at large redshifts, namely [34]:

$$\frac{H^2}{(H_0^*)^2} = \Omega_m^*\left(a^{-3} + X^* a^{-4}\right) + \Omega_\Lambda^*, \qquad \frac{R}{2\Lambda} = 2 + \frac{\Omega_m^*}{2\Omega_\Lambda^*}a^{-3}, \qquad a \to 0. \tag{7}$$

Here the index $*$ refers to parameters as given in the ΛCDM model. In particular, $\Omega_\Lambda^* = \frac{\Lambda}{3(H_0^*)^2}$ and H_0^* is the Hubble constant in the ΛCDM scenario as measured today. However, the late-time evolution for the $F(R)$ models deviates from these initial conditions and consequently from ΛCDM model, such that the above parameters measured today for our models will be different:

$$H_0 \neq H_0^*, \qquad \Omega_m^0 \neq \Omega_m^* ,$$

Nevertheless, these parameters are connected among themselves [28, 34]:

$$\Omega_m^0 H_0^2 = \Omega_m^*(H_0^*)^2 = \frac{\kappa^2}{3}\rho_m(t_0), \qquad \Omega_\Lambda H_0^2 = \Omega_\Lambda^*(H_0^*)^2 = \frac{\Lambda}{3} . \tag{8}$$

It is also convenient as shown below, to redefine the Hubble parameter and the Ricci scalar as dimensionless functions:

$$E = \frac{H}{H_0^*}, \qquad \mathcal{R} = \frac{R}{2\Lambda} . \tag{9}$$

The first model is given by the following exponential function [31, 34, 36, 40]:

$$F(R) = R + F_{\text{DE}} = R - 2\Lambda\left[1 - \exp\left(-\beta\frac{R}{2\Lambda}\right)\right] . \tag{10}$$

Note that this exponential model turns out ΛCDM model at the limit $\beta \to \infty$. Moreover, at large redshifts, the model also recovers ΛCDM as the curvature becomes large enough $R >> \Lambda/\beta$. Hence, physical solutions for this $F(R)$ action tend asymptotically to ΛCDM solutions at large redshifts, such that the above initial conditions (7) results convenient for the equations. By using the dimensionless variables defined in (9), the corresponding system of equations (3) can be rewritten as:

$$\begin{aligned}
\frac{dE}{d\log a} &= \Omega_\Lambda^*\frac{\mathcal{R}}{E} - 2E , \\
\frac{d\mathcal{R}}{d\log a} &= \frac{e^{\beta\mathcal{R}}}{\beta^2}\left[\Omega_m^*\frac{a^{-3} + X_r a^{-4}}{E^2} - 1 + \beta e^{-\beta\mathcal{R}} + \Omega_\Lambda^*\frac{1 - (1 + \beta\mathcal{R})\,e^{-\beta\mathcal{R}}}{E^2}\right] .
\end{aligned} \tag{11}$$

This system of equations can be solved by integrating over the independent variable $x = \log a = -\log(z + 1)$ and assuming the initial conditions (7) at the point x_i, where $e^{-\beta\mathcal{R}(x_i)} \in (10^{-9}, 10^{-7})$ and our model mimics ΛCDM (for more details see Ref. [34]). Then, we confront the model with the observational data by fitting the free parameters and keeping in mind that $H(z) = H_0^*E(z)$ with the true value for the Hubble parameter today being $H_0 = H_0^*E(z = 0)$ and also the relation (8) for the matter density.

Following the same procedure, a second $F(R)$ model with a power-law of the Ricci scalar is analysed, which is described by the gravitational action [37–39]:

$$F(R) = R - 2\Lambda\gamma\left(\frac{R}{2\Lambda}\right)^\delta + F_{\text{EDE}}, \qquad F_{\text{EDE}} = -\alpha \cdot 2\Lambda R_0^\ell \frac{R^{m-n}R^n}{R_0^{\ell+m} + R^{\ell+m}} \tag{12}$$

Note that here the so-called early dark energy (EDE) term F_{EDE} is included where α, ℓ, m, n, R_0 are constants, and the curvature scale R_0 corresponds to the Ricci scalar value for the epoch $1000 \leq z \leq 3000$ (see Ref. [37]). This term can generate a quasi-stable de Sitter stage at $R = R_0$ as far as n is an odd integer, and ℓ, m are large enough in absence of matter. However, in the presence of matter, the limitations on the parameters ℓ, m, n are connected with the behavior of F_{RR} in Eq. (12).

By considering the model (12) without the EDE term ($\alpha = 0$), the model does not recover purely the ΛCDM model at the limit $R \to \infty$. However, this power-law model may mimic the ΛCDM asymptotic behavior (7) at large curvature

$10 \leq \mathcal{R} \leq 10^{10}$, whose solutions are free of divergences and singularities. In this approach we can numerically solve the system of equations (3) by fixing the initial conditions (7) at large redshifts, corresponding to $1000 \leq z \leq 3000$. The system of equations (3) for this case ($\alpha = 0$) yields:

$$
\begin{aligned}
\frac{dE}{d \log a} &= \Omega_\Lambda^* \frac{\mathcal{R}}{E} - 2E \ , \\
\frac{d \log \mathcal{R}}{d \log a} &= \frac{\mathcal{R}^{1-\delta}}{\gamma(1-\delta)} \left[\frac{\Omega_m^*(a^{-3} + X_r a^{-4}) + \Omega_\Lambda^* \gamma \delta (1-\delta) \mathcal{R}^\delta}{E^2} - 1 \right] + \frac{1}{1-\delta} \ .
\end{aligned}
\tag{13}
$$

By solving these equations, the corresponding solutions show an undesirable oscillatory behavior at large R (see Refs. [37, 39]), especially in the most interesting limit $\delta \ll 1$. An example of these oscillations is depicted in Fig. 1. Such behavior may be controlled via a choice of the initial conditions (they were optimized in the case shown in the figure) but can not be completely suppressed in the framework of this model.
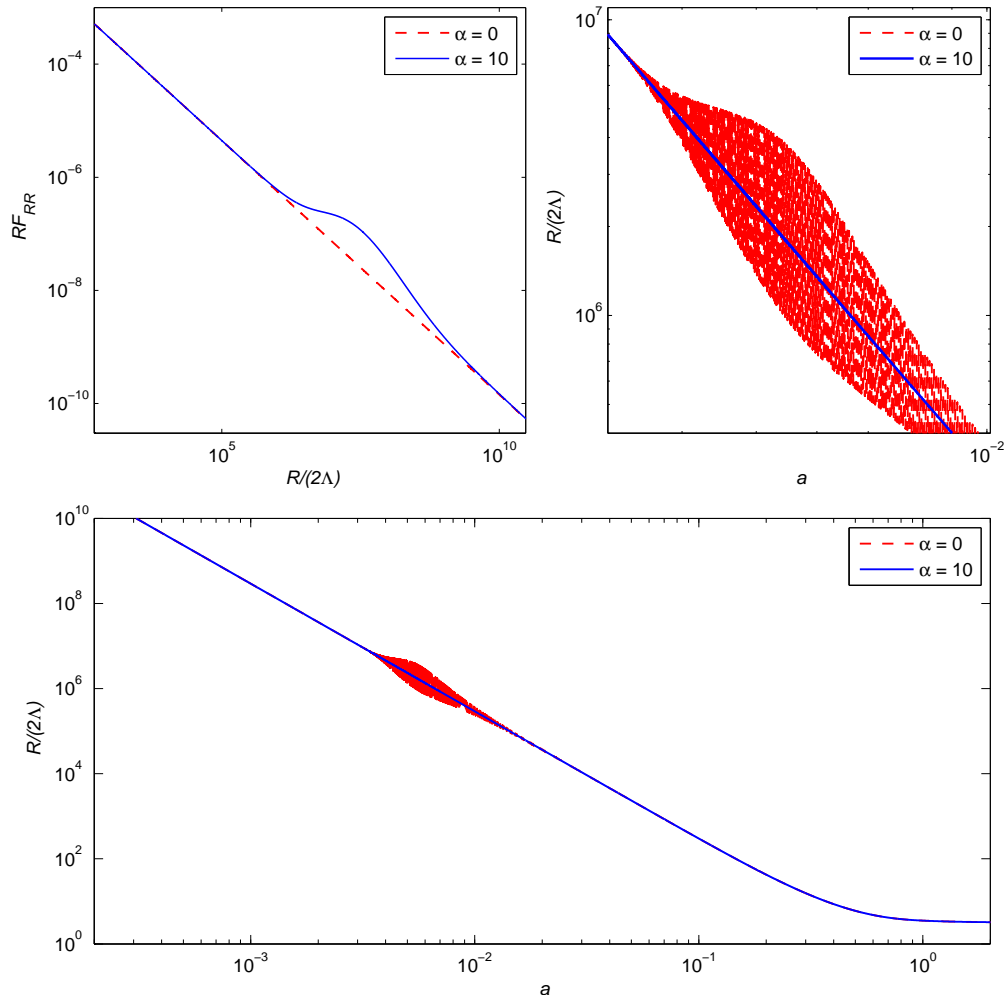

FIG. 1: Power-law model (12) with $\alpha = 0$ (dashed lines) and with $\alpha = 10$ (solid lines): plots for $RF_{RR}(\mathcal{R})$ (top-left panel) and solutions $\mathcal{R}(a)$ for $\gamma = 1.5$, $\delta = 0.1$, $\mathcal{R}_0 = 2 \cdot 10^7$, $m = 1$, $\ell = n = 0$, $\Omega_0 = 0.26$.

Nevertheless, by including the EDE term, these oscillations can be effectively suppressed, that is with a regular evolution for $\mathcal{R}$ and H. Nevertheless, one should note that for $n \geq 1$ and (or) $\ell \geq 1$ the second derivative of $F_{\mathrm{EDE}}(R)$ changes its sign many times close to $R = R_0$, so $F_{RR}(R)$ in the denominator of Eq. (3) can lead to singularities if α is not small enough. Due to this reason, if the numbers n, m or ℓ are large, the value for α should be small. In this case, F_{EDE} practically does not influence on describing observational data. Nevertheless, for the case $m = 1$, $\ell = n = 0$, the corresponding EDE term becomes:

$$
F_{\mathrm{EDE}} = -2\Lambda\alpha \frac{R}{R_0 + R} \ .
\tag{14}
$$

And the denominator $F_{RR}(R)$ in Eq. (3) behaves well for such a case (see the top-left panel in Fig. 1) and we can use this term with rather large α to suppress oscillations during the epoch when $R \simeq R_0$ and later. Figure 1 also depicts the evolution of the Ricci scalar for this choice.

Thus, non-oscillating and non-diverging solutions of the model (12) with the EDE term (14) can be obtained and confronted with the observational data.

III. OBSERVATIONAL DATA

Here we are interested to confront the models described in the previous section in order to obtain the best fit for the free parameters and particularly the best fit for H_0 when using different data sources. As mentioned above, these observations include: (a) Type Ia supernovae (SNe Ia) data from Pantheon sample [45]; (b) estimates of the Hubble parameter $H(z)$ from cosmic chronometers and line-of-sight BAO and (c) CMB data from Planck 2018 [3, 46].

For the SNe Ia we use the Pantheon sample database [45] with $N_{\mathrm{SN}} = 1048$ points and compare the corresponding SNe Ia distance moduli μ_i^{obs} at redshift z_i from the catalog with their theoretical values by minimizing the χ^2 function:

$$\chi_{\mathrm{SN}}^2(p_1, \dots) = \min_{H_0} \sum_{i,j=1}^{N_{\mathrm{SN}}} \Delta\mu_i \big(C_{\mathrm{SN}}^{-1}\big)_{ij} \Delta\mu_j, \qquad \Delta\mu_i = \mu^{th}(z_i, p_1, \dots) - \mu_i^{obs} , \tag{15}$$

Here C_{SN} is the covariance matrix [45] and p_j are the free model parameters, whereas the distance moduli is given by:

$$\mu^{th}(z) = 5 \log_{10} \frac{D_L(z)}{10\mathrm{pc}}, \qquad D_L(z) = (1+z)\, D_M, \qquad D_M(z) = c \int\limits_0^z \frac{d\tilde{z}}{H(\tilde{z})}$$

In the expression (15) the Hubble constant H_0 is considered as a nuisance parameter [34, 35, 41–43] for SNe Ia data, so can be marginalized and estimations can not be obtained for H_0 from χ_{SN}^2. However, this provides very important information when fitting the other model parameters.

On the other hand, the Hubble parameter data $H(z)$ are obtained by two different ways of estimation [34, 35, 41–44]. The first one is the cosmic chronometers (CC), i.e. estimations of $H(z)$ by using galaxies of different ages Δt located closely in terms of the redshift Δz,

$$H(z) = \frac{\dot{a}}{a} = -\frac{1}{1+z} \frac{dz}{dt} \simeq -\frac{1}{1+z} \frac{\Delta z}{\Delta t}.$$

Here we consider 31 CC $H(z)$ data points given in Ref. [47]. In the second method $H(z)$ values are estimated from the baryon acoustic oscillation (BAO) data along the line-of-sight direction. In this paper we use 36 $H_{\mathrm{BAO}}(z)$ data points from Refs. [48, 49] that can be found in [50]. For a particular cosmological model with free parameters $p_1, p_2, \dots$, we calculate the χ^2 function by using the CC $H(z)$ data and the full set CC + H_{BAO} separately, as follows: function

$$\chi_H^2(p_1, \dots) = \sum_{j=1}^{N_H} \left[\frac{H(z_j, p_1, \dots) - H^{obs}(z_j)}{\sigma_j} \right]^2 \tag{16}$$

Note that H_{BAO} data points are correlated with BAO angular distances, such that are not considered in other analysis (see Refs. [34, 35, 41]). Nevertheless, here we do not use BAO angular distances, such that we avoid any correlation.

The last source used along the paper is the data from the cosmic microwave background radiation (CMB) that are given by the following observational parameters [46]

$$\mathbf{x} = \big(R, \ell_A, \omega_b\big), \qquad R = \sqrt{\Omega_m^0} \frac{H_0 D_M(z_*)}{c}, \qquad \ell_A = \frac{\pi D_M(z_*)}{r_s(z_*)}, \qquad \omega_b = \Omega_b^0 h^2 , \tag{17}$$

where $z_* = 1089.80 \pm 0.21$ is the photon-decoupling redshift [3], while $h = H_0/[100\,\mathrm{km s^{-1} Mpc^{-1}}]$, the radiation-matter ratio $X_r = \Omega_r^0/\Omega_m^0$ is given in (6), and we consider the current baryon fraction Ω_b^0 as the nuisance parameter to marginalize over. The corresponding χ^2 function is:

$$\chi_{\mathrm{CMB}}^2 = \min_{\omega_b} \Delta\mathbf{x} \cdot C_{\mathrm{CMB}}^{-1} \big(\Delta\mathbf{x}\big)^T, \qquad \Delta\mathbf{x} = \mathbf{x} - \mathbf{x}^{Pl} . \tag{18}$$

where [46]

$$\mathbf{x}^{Pl} = \left(R^{Pl}, \ell_A^{Pl}, \omega_b^{Pl}\right) = \left(1.7428 \pm 0.0053, \ 301.406 \pm 0.090, \ 0.02259 \pm 0.00017\right) , \tag{19}$$

with free amplitude for the lensing power spectrum, from Planck collaboration 2018 data [3]. The covariance matrix $C_{\mathrm{CMB}} = \|\tilde{C}_{ij}\sigma_i\sigma_j\|$, the expression $r_s(z_*)$ and other details are well described in Refs. [35, 41] and [46].

IV. RESULTS AND DISCUSSION

Let us now fit the corresponding models parameters through the χ^2 functions as given in (15),(16) and (18) for each $F(R)$ model. We consider separately the SNe Ia and $H(z)$ CC (or CC + H_{BAO}) data,

$$\chi^2_{\mathrm{SN}+H} = \chi^2_{\mathrm{SN}} + \chi^2_H \tag{20}$$

and the same SNe Ia and $H(z)$ data with the CMB contribution (18)

$$\chi^2_{\mathrm{SN}+H+\mathrm{CMB}} = \chi^2_{\mathrm{SN}} + \chi^2_H + \chi^2_{\mathrm{CMB}} . \tag{21}$$

We follow this procedure as the CMB data (18) with narrow priors (19) produce the most tight limitations on the model parameters, particularly on the density matter parameter due to the factor $\sqrt{\Omega_m^0}$ in Eq. (17) (see Fig. 2). Thus, for the two $F(R)$ models we analyze four different sets of data:

$$\begin{array}{ll} \text{SNe Ia + CC,} & \text{SNe Ia + CC} + H_{\mathrm{BAO}}; \\ \text{SNe Ia + CC + CMB,} & \text{SNe Ia + CC} + H_{\mathrm{BAO}} + \text{CMB.} \end{array} \tag{22}$$

Following the way of maximizing the likelihood, we obtain the corresponding distributions and contour plots for the free parameters for both $F(R)$ models.

The exponential model (10) owns four free parameters: H_0, Ω_m^0, Ω_Λ, β or equivalently H_0^*, Ω_m^*, Ω_Λ^*, β. However, Ω_Λ may be considered as a conditionally free parameter because the χ^2 functions (20) and (21) have sharp minimums along the line $\Omega_m^0 + \Omega_\Lambda \simeq \xi(\beta)$, where $\xi(\beta) \to 1$ in the ΛCDM limit $\beta \to \infty$. Figure 2 depicts the contours at 1σ (68.27%), 2σ (95.45%) and 3σ (99.73%) for the four data sets given in (22) when considering the exponential model (10). The planes $H_0 - \Omega_m^0$ and $H_0 - \beta$ are obtained by maximizing the likelihood (minimizing the χ^2) over the other parameters, while the absolute maximums are described by circles, stars etc. The right panels depict the same contour plots but with additional details, in particular, the second one is re-scaled along the Ω_m^0 axis. The corresponding one-parameter distributions shown in the top left panel corresponds to the likelihood function for H_0 after maximizing over the other parameters:

$$\mathcal{L}_j(H_0) \sim \exp(-\chi_j^2(H_0)/2) . \tag{23}$$

Following the same procedure, the fits of the free parameters for the power-law model (12) with the EDE term (14) are obtained by the data sets (22). This model has the free parameters: H_0, Ω_m^0, Ω_Λ, γ, δ, α and R_0. Although the EDE factor α is denoted by $\alpha^* = \log\alpha$ in Table II. We fix $R_0/(2\Lambda) = 1.2 \cdot 10^{-7}$ corresponding to the epoch before or near the recombination and work with the remaining 6 parameters. Here Ω_Λ can be considered as a conditionally free parameter, because the functions $\chi_j^2(\Omega_\Lambda, \dots)$ behave like in the previous exponential model. The 1σ and 2σ contour plots are shown in Fig. 3. In these contour plots and in the likelihood functions (23) we also minimize χ_j^2 over the other parameters.

Table II summarizes the results for both $F(R)$ models together with ΛCDM model, where the minimum χ^2, the best fits of the free parameters and their errors are shown for the different data sets considered here (22). We can evaluate the three models in Table II from the point of view of information criteria depending on the number N_p of the free model parameters. In this sense, the Akaike information criterion [51] $AIC = \min\chi^2_{tot} + 2N_p$ provides a way to compare the goodness of the fits. Then, ΛCDM model with $N_p = 2$ gives a better estimation in comparison with the exponential $F(R)$ model with $N_p = 4$ and the power-law model with $N_p = 6$. On the other hand, the minimum χ_j^2 for the exponential model (10) shows a better fit than ΛCDM model for the four sets (22), with the largest difference for the SNe Ia + CC + H_{BAO} data, where additionally the 1σ region for the β parameter does not include ΛCDM model (recall that this is recovered for $\beta \to \infty$). The other three sets show similar fits, including ΛCDM model within the errors for β. The value of H_0 for the best fit depends on the data set, with its maximum given by $H_0 = 70.28 \pm 1.6$ km s^{-1}Mpc^{-1} (SNe Ia + CC + CMB) and its minimum by $H_0 = 68.15^{+1.21}_{-1.20}$ km s^{-1}Mpc^{-1}
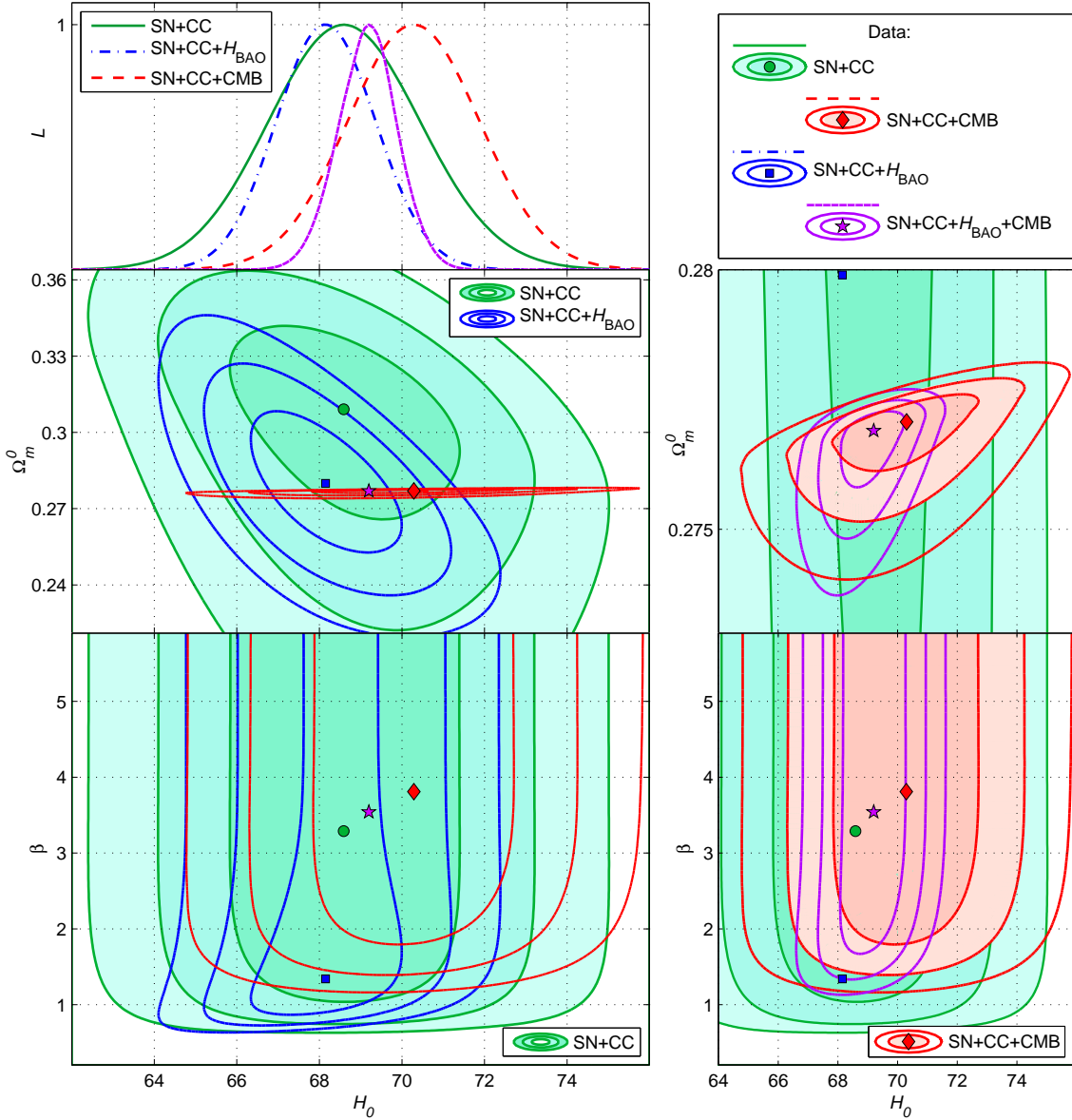
FIG. 2: Exponential model (10): 1σ, 2σ and 3σ CL contour plots for $\chi^2(H_0, \Omega_m^0)$, $\chi^2(H_0, \beta)$ and likelihood functions $\mathcal{L}_H(H_0)$ for the 4 sets of observational data.

(SNe Ia + CC + H_{BAO}).

One can see that for the power-law model (12), which owns 6 free parameters, the absolute minimum min χ_j^2 is similar in comparison with the exponential $F(R)$ and the ΛCDM models for all data sets (22), with a slightly better fit for the case with for SNe Ia + CC + H_{BAO} data. This may be explained as follows: only in this case the best fit value for the parameter $\delta = 0.17^{+0.11}_{-0.095}$ is large enough for an effective role of the dark energy $F(R)$ term in this model (12). While the other data sets (22), especially for SNe Ia + CC + H_{BAO} data, the best fit for δ is close to zero, but as far as $\delta \to 0$ the power-law model (12) tends to the ΛCDM model and the EDE term should be strongly limited.

Concerning the H_0 tension problem, Table II also gathers the estimations for the Hubble constant for both $F(R)$ models and ΛCDM model when confronting the models with the data sets given in (22). By a first look, the best fit values for H_0 are very similar for both the exponential model (10) as for the power-law model (12), such that they are depicted together in the box plots of Fig. 4. Moreover, these estimations are very close to the ΛCDM model predictions for three combinations of the observational data (22), whereas for the case SNe Ia + CC + H_{BAO}, error bars are larger for the $F(R)$ models and the best fit value is shifted to smaller values of H_0. As shown in Table II, the case SNe Ia + CC + H_{BAO} gives the most disparate results when compared to ΛCDM model, as the errors on
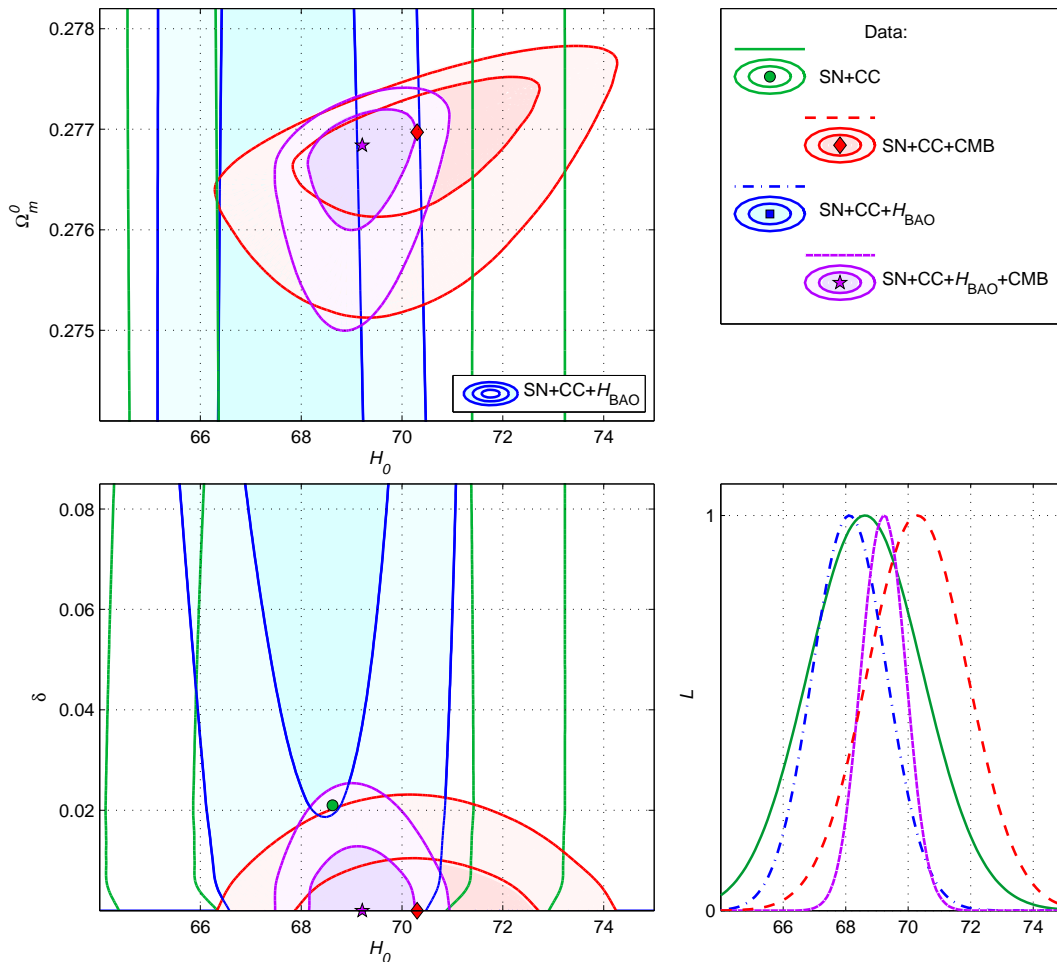
FIG. 3: Power-law model (12) with the EDE term: 1σ and 2σ CL contour plots in $H_0 - \Omega_m^0$, $H_0 - \delta$ planes and likelihood functions $\mathcal{L}_j(H_0)$.

the free parameters does not include ΛCDM model within the error bars in both $F(R)$ models. The same applies to the Ω_m^0 parameter, which is almost the same value for three of the data sets, and slightly different for the SNe Ia + CC + $H_{\rm BAO}$ set. In addition, the inclusion of CMB data implies much smaller errors on the matter density parameter, as natural due to the factor appearing in (17).

Hence, the results draw an scenario that despite the H_0 tension is not alleviated in the $F(R)$ models, it gives an interesting result when considering the SNe Ia + CC + $H_{\rm BAO}$ data set, as excludes ΛCDM from the 1σ region.

V. CONCLUSIONS

In this paper we have explored two $F(R)$ gravity models, where the cosmological evolution is obtained by solving a dynamical system of equations and then compare to observational data. The models explored along this paper consist of an exponential correction to the Hilbert-Einstein action (10) and the power-law model (12) with the EDE term (14). Keeping in mind their capabilities in alleviating the H_0 tension between the Planck [3] and SH0ES [5] estimations of H_0, these models were confronted with observational data including SNe Ia, 2 types of $H(z)$ estimations and CMB data, and by combining this data in four different sets in order to analyze the differences and the possible biased introduced by some of the sets on the parameter estimations.

The results are summarized in Table II, which shows the best fits for the Hubble constant H_0. As discussed along the paper, the values obtained for each model are very similar, with no particular differences among the $F(R)$ models. In the box plot depicted in Fig. 4, the 1σ error for both $F(R)$ gravities is the same, and in

Model	Data	min $\chi^2/d.o.f$	H_0	Ω_m^0	other parameters
Expon. $F(R)$	SN+CC	1072.78 /1076	$68.59^{+1.85}_{-1.82}$	$0.309^{+0.0215}_{-0.0255}$	$\beta = 3.29^{+\infty}_{-1.92}$
	SN+CC+$H_{\rm BAO}$	1081.33 /1112	$68.15^{+1.21}_{-1.20}$	$0.2799^{+0.0186}_{-0.018}$	$\beta = 1.34^{+0.99}_{-0.36}$
	SN+CC+CMB	1083.70 /1079	$70.28^{+1.60}_{-1.60}$	$0.2771^{+0.0004}_{-0.0005}$	$\beta = 3.80^{+\infty}_{-1.62}$
	SN+all H+CMB	1091.88 /1115	$69.22^{+0.66}_{-0.73}$	$0.2769^{+0.0003}_{-0.0006}$	$\beta = 3.52^{+\infty}_{-1.54}$
Power-law + EDE	SN+CC	1072.78 /1074	$68.62^{+1.85}_{-1.83}$	$0.311^{+0.0295}_{-0.038}$	$\delta = 0.021^{+0.215}_{-0.019}, \ \alpha^* = 10.78^{+0.64}_{-1.13}$
	SN+CC+$H_{\rm BAO}$	1080.27 /1110	$68.20^{+1.14}_{-1.35}$	$0.2635^{+0.0142}_{-0.0125}$	$\delta = 0.17^{+0.11}_{-0.095}, \ \alpha^* = 10.32^{+1.33}_{-1.27}$
	SN+CC+CMB	1083.77 /1077	$70.29^{+1.61}_{-1.60}$	$0.2770^{+0.0004}_{-0.0005}$	$\delta = 0.001^{+0.005}_{-0.001}, \ \alpha^* \leq 4.6$
	SN+all H+CMB	1092.02 /1113	$69.23^{+0.67}_{-0.75}$	$0.2768^{+0.0003}_{-0.0004}$	$\delta = 0.001^{+0.007}_{-0.001}, \ \alpha^* \leq 3.9$
ΛCDM	SN+CC	1072.80 /1078	$68.60^{+1.84}_{-1.84}$	$0.3095^{+0.0211}_{-0.0205}$	$\Omega_\Lambda = 1 - \Omega_m^0$
	SN+CC+$H_{\rm BAO}$	1083.06 /1114	$68.52^{+1.20}_{-1.20}$	$0.2883^{+0.0172}_{-0.0163}$	
	SN+CC+CMB	1083.77 /1081	$70.28^{+1.61}_{-1.59}$	$0.2771^{+0.0003}_{-0.0003}$	
	SN+all H+CMB	1092.05 /1117	$69.21^{+0.71}_{-0.69}$	$0.2769^{+0.0002}_{-0.0002}$	

TABLE II: The best fit values for H_0 (in $\rm km\,s^{-1}Mpc^{-1}$) and other parameters for the cosmological scenarios: the exponential $F(R)$ model (10) and the power-law model (12) in comparison with the ΛCDM model.
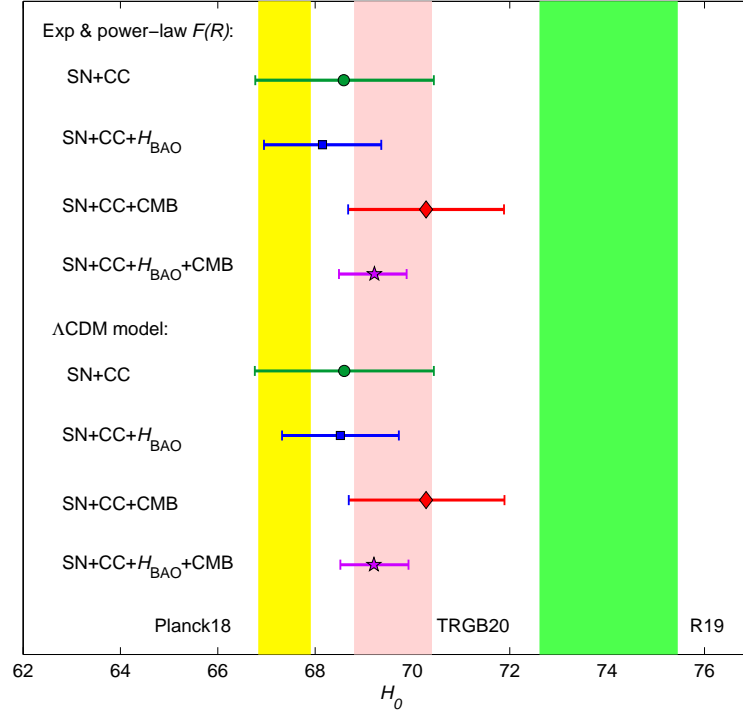

FIG. 4: Box plots for the exponential and power-law $F(R)$ models, together with the ΛCDM model in comparison with Planck18, TRGB20 and SH0ES (R19) H_0 estimations.

comparison with the one from the ΛCDM model, are also very close for the all data sets (22). The H_0 estimations for the two $F(R)$ models are close to the ΛCDM model. Moreover, the best fits for three of the data sets are achieved within the range where the $F(R)$ models tend asymptotically to ΛCDM, i.e. $\beta \to \infty$ for the exponential model (12) and $\delta \to 0$ for the power-law model (12). Nevertheless, for the SNe Ia + CC + $H_{\rm BAO}$ data set, both $F(R)$ models do not include ΛCDM model within the 1σ region, and the best fits in terms of the minimum value of χ^2 shows a goodness of the fits much better than ΛCDM model, and better than the other data sets.

In addition, as shown in Fig. 4, where the vertical bands refer to H_0 estimations from Planck 2018 release [3], SH0ES (HST) group [5] and the intermediate recent value by CCHP group with the red giant branch (TRGB) method [9], the H_0 tension does not show a better behavior within these $F(R)$ models but the tension problem remains. In particular, while the data sets that excludes CMB data fit well the estimations for H_0 from Planck 2018

and TRGB, it does not when CMB rulers is included. The same applies to the ΛCDM model, as shown in Fig. 4.

Hence, we may conclude that the $F(R)$ models considered in the paper, described by the gravitational actions given in (10) and (12), can not exhaustively explain the tension between the Planck [3] and SH0ES [5] H_0 estimations, but they can alleviate this tension to some extent. The most interesting result lies on the analysis of both $F(R)$ models with SNe Ia + CC + $H_{\rm BAO}$ data set, as excludes the ΛCDM limit from the best fit region, a possible signal of the deviations from ΛCDM and/or of the issue of the data sets.

Acknowledgements

[1] Planck Collaboration, P. A. R. Ade et al. Astron. Astrophys. 571 (2014) A16, arXiv:1303.5076.

[2] Planck Collaboration, P. A. R. Ade et al. Astron. Astrophys. 594 (2016) A13, arXiv:1502.01589.

[3] Planck Collaboration, N. Aghanim et al. *Planck 2018 results. VI. Cosmological parameters.* arXiv:1807.06209.

[4] A. G. Riess, S. Casertano, W. Yuan et al., Astrophys J. 861 (2018) 126, arXiv: 1804.10655.

[5] A. G. Riess, S. Casertano, W. Yuan, L. M. Macri and D. Scolnic, Astrophys J. 876 (2019) 85, arXiv: 1903.07603.

[6] L. Verde, T. Treu and A. G. Riess, Nature Astronomy 3 (2019) 891, arXiv:1907.10625.

[7] E. Di Valentino, L. A. Anchordoqui, Y. Ali-Haimoud et al., Cosmology Intertwined II: The Hubble Constant Tension, arXiv:2008.11284.

[8] W. L. Freedman, B. F. Madore, D. Hatt et al., Astrophys J. 882 (2019) 34, arXiv:1907.05922.

[9] W. L. Freedman B. F. Madore, T. Hoyt et al., arXiv:2002.01550.

[10] K. C. Wong, S. H. Suyu, G. C.-F. Chen et al., 2019, Mon. Not. Roy. Astron. Soc., doi:10.1093/mnras/stz3094, arXiv:1907.04869.

[11] J.-J. Wei and F. Melia, Astrophys.J. 897 (2020) 2, 127, arXiv:2005.10422.

[12] P. Denzel, J. P. Coles, P. Saha and L. L. R. Williams, The Hubble constant from eight time-delay galaxy lenses, arXiv:2007.14398.

[13] E. J. Baxter and B. D. Sherwin, arXiv:2007.04007.

[14] D. W. Pesce, J. A. Braatz, M. J. Reid, A. G. Riess et al., 2020, Astrophys. J. Lett., 891 (2020) L1, arXiv:2001.09213.

[15] C. D. Huang, A. G. Riess, W. Yuan et al., 2019, Astrophys. J. 889 (2020) 1, 5, arXiv:1908.10883.

[16] G. E. Addison, Y. Huang, D. J. Watts et al., Astrophys. J. 818 (2016) 132, arXiv:1511.00055; M. Lattanzi, C. Burigana, M. Gerbino et al., JCAP 1702 (2017) 041, arXiv:1611.01123; Y. Huang, G. E. Addison, J. L. Weiland and C. L. Bennett, Astrophys. J. 869 (2018) 38, arXiv:1804.05428. D. O. Jones, A. G. Riess, D. M. Scolnic et al., Astrophys. J. 867 (2018) 108, arXiv:1805.05911; W. D. Kenworthy, D. Scolnic and A. Riess, Astrophys. J. 875 (2019) 145, arXiv:1901.08681; M. Martinelli and I. Tutusaus, Symmetry 11 (2019) 8, 986, arXiv:1906.09189; S. A. Vallejo-Peña and A. E. Romano, JCAP 2003 (2020) 023, arXiv:1906.04946.

[17] Q.-G. Huang and K. Wang, Eur. Phys. J. C76 (2016) 506, arXiv:1606.05965; E. Di Valentino, A. Melchiorri, E. V. Linder and J. Silk, Phys. Rev. D. 96 (2017) 023523, arXiv:1704.00762; W. Yang, S. Pan and A. Paliathanasis, Mon. Not. Roy. Astron. Soc. 475 (2018) 2605, arXiv:1708.01717; W. Yang, S. Pan, E. Di Valentino, E. N. Saridakis and S. Chakraborty, Phys. Rev. D. 99 (2019) 043543, arXiv:1810.05141; W. Yang, S. Pan, E. Di Valentino and E. N. Saridakis, Universe 5 no. 11 (2019) 219, arXiv:1811.06932; R. E. Keeley, S. Joudaki, M. Kaplinghat and D. Kirkby, JCAP 12 (2019) 035, arXiv:1905.10198; E. Di Valentino, A. Melchiorri and J. Silk, JCAP 01 (2020) 013, arXiv:1908.01391; E. Di Valentino, A. Mukherjee, and A. A. Sen, arXiv:2005.12587; X. Li and A. Shafieloo, Astrophys. J. Lett. 883 no. 1, (2019) L3, arXiv:1906.08275; M. Rezaei, T. Naderi, M. Malekjani, and A. Mehrabi, Eur. Phys. J. C. 80 no. 5, (2020) 374, arXiv:2004.08168;

[18] V. Poulin, T. L. Smith, T. Karwal and M. Kamionkowski, Phys. Rev. Lett. 122 no. 22, (2019) 221301, arXiv:1811.04083. E. Mörtsell and S. Dhawan, JCAP 1809 (2018) 025, arXiv:1801.07260; J. Sakstein and M. Trodden, Phys. Rev. Lett. 124 (2020) 161301, arXiv:1911.11760; F. Niedermann and M. S. Sloth, arXiv:1910.10739.

[19] Z. Berezhiani, A. Dolgov and I. Tkachev, Phys. Rev. D. 92 (2015) 061303, arXiv:1505.03644; A. Chudaykin, D. Gorbunov, and I. Tkachev, Phys. Rev. D. 97 (2018) 083508, arXiv:1711.06738; K. L. Pandey, T. Karwal and S. Das, JCAP 07 (2020) 026, sarXiv:1902.10636; K. Vattis, S. M. Koushiappas and A. Loeb, Phys. Rev. D. 099 (2019) 121302, arXiv:1903.06220; A.Hryczuk,and K. Jodlowski, Phys. Rev. D. 102 (2020) 043024, arXiv:2006.16139.

[20] E. Di Valentino, A. Melchiorri and O. Mena Phys. Rev. D. 96 (2017) 043503, arXiv:1704.08342; W. Yang, S. Pan, E. Di Valentino, R. C. Nunes, S. Vagnozzi and D. F. Mota, JCAP 1809 (2018) 019, 21 arXiv:1805.08252: W. Yang, A. Mukherjee, E. Di Valentino and S. Pan, Phys. Rev. D. 98 (2018) 123527, arXiv:1809.06883; S. Kumar, R. C. Nunes and S. K. Yadav, Eur. Phys. J. C. 79 (2019), 576, arXiv:1903.04865; S. Pan, W. Yang, C. Singha and E. N. Saridakis Phys. Rev. D. 100 (2019) 083539, arXiv:1903.10969; S. Pan, W. Yang, E. Di Valentino, E. N. Saridakis and S. Chakraborty, Phys. Rev. D. 100 (2019) 103520, arXiv:1907.07540; E. Di Valentino, A. Melchiorri, O. Mena and S. Vagnozzi, Phys. Dark Univ. 30 (2020)

100666, arXiv:1908.04281; E. Di Valentino, A. Melchiorri, O. Mena and S. Vagnozzi, Phys. Rev. D. 101 (2020) 063502, arXiv:1910.09853; A. Gomez-Valent, V. Pettorino and L. Amendola, Phys. Rev. D 101 (2020) 123513, arXiv:2004.00610; S. Pan, G. S. Sharov and W. Yang, Phys. Rev. D 101 (2020) 10, 103533, arXiv:2001.03120.

[21] F. D'Eramo, R. Z. Ferreira, A. Notari and J. L. Bernal, JCAP 1811 (2018) 014, arXiv:1808.07430; S. Carneiro, P. C. de Holanda, C. Pigozzo, and F. Sobreira, Phys. Rev. D. 100 (2019) 023505, arXiv:1812.06064; S. Vagnozzi, Phys. Rev. D. 102 (2020) 023518, arXiv:1907.07569; K.-F. Lyu, E. Stamou and L.-T. Wang, arXiv:2004.10868; F. Arias-Aragon, E. Fernandez-Martinez, M. Gonzalez-Lopez and L. Merlo, arXiv:2009.01848.

[22] R. C. Nunes, JCAP 1805 (2018) 052, arXiv:1802.02281; D. Wang and D. Mota, arXiv:2003.10095; M. Ballardini, M. Braglia, F. Finelli, D. Paoletti, A. A. Starobinsky and C. Umilta, arXiv:2004.14349,

[23] D. Wang, arXiv:2008.03966.

[24] M. Zumalacarregui, Phys. Rev. D **102** (2020) no.2, 023523 doi:10.1103/PhysRevD.102.023523 [arXiv:2003.06396 [astro-ph.CO]].

[25] S. Nojiri and S. D. Odintsov, Phys. Rept. **505**, 59-144 (2011) doi:10.1016/j.physrep.2011.04.001 [arXiv:1011.0544 [gr-qc]]; S. Nojiri, S. D. Odintsov and V. K. Oikonomou, Phys. Rept. **692**, 1-104 (2017) doi:10.1016/j.physrep.2017.06.001 [arXiv:1705.11098 [gr-qc]]. G. J. Olmo, Int. J. Mod. Phys. D **20**, 413-462 (2011) doi:10.1142/S0218271811018925 [arXiv:1101.3864 [gr-qc]]. S. Capozziello and M. De Laurentis, Phys. Rept. **509**, 167-321 (2011) doi:10.1016/j.physrep.2011.09.003 [arXiv:1108.6266 [gr-qc]]; S. Capozziello, T. Harko, T. S. Koivisto, F. S. N. Lobo and G. J. Olmo, Universe **1**, no.2, 199-238 (2015) doi:10.3390/universe1020199 [arXiv:1508.04641 [gr-qc]]. T. Clifton, P. G. Ferreira, A. Padilla and C. Skordis, Phys. Rept. **513**, 1-189 (2012) doi:10.1016/j.physrep.2012.01.001 [arXiv:1106.2476 [astro-ph.CO]]; A. de la Cruz-Dombriz and D. Saez-Gomez, Entropy **14**, 1717-1770 (2012) doi:10.3390/e14091717 [arXiv:1207.2663 [gr-qc]].

[26] S. Capozziello, Int. J. Mod. Phys. D **11**, 483-492 (2002) doi:10.1142/S0218271802002025 [arXiv:gr-qc/0201033 [gr-qc]]; S. Nojiri and S. D. Odintsov, Phys. Rev. D **68**, 123512 (2003) doi:10.1103/PhysRevD.68.123512 [arXiv:hep-th/0307288 [hep-th]]; S. Nojiri and S. D. Odintsov, Phys. Rev. D **74**, 086005 (2006) doi:10.1103/PhysRevD.74.086005 [arXiv:hep-th/0608008 [hep-th]]; D. Saez-Gomez, Gen. Rel. Grav. **41**, 1527-1538 (2009) doi:10.1007/s10714-008-0724-3 [arXiv:0809.1311 [hep-th]]; E. Elizalde and D. Saez-Gomez, Phys. Rev. D **80**, 044030 (2009) doi:10.1103/PhysRevD.80.044030 [arXiv:0903.2732 [hep-th]]; N. Goheer, J. Larena and P. K. S. Dunsby, Phys. Rev. D **80**, 061301 (2009) doi:10.1103/PhysRevD.80.061301 [arXiv:0906.3860 [gr-qc]];

[27] S. D. Odintsov, V. K. Oikonomou and F. P. Fronimos, Phys. Dark Univ. 29 (2020) 100563, arXiv:2004.08884/

[28] W. Hu and I. Sawicki, Phys. Rev. D 76 (2007) 064004, arXiv:0705.1158.

[29] S. Nojiri and S. D. Odintsov, Phys. Lett. B **657**, 238-245 (2007) doi:10.1016/j.physletb.2007.10.027 [arXiv:0707.1941 [hep-th]].

[30] Á. de la Cruz-Dombriz, P. K. S. Dunsby, S. Kandhai and D. Sáez-Gómez, Phys. Rev. D **93**, no.8, 084016 (2016) doi:10.1103/PhysRevD.93.084016 [arXiv:1511.00102 [gr-qc]].

[31] K. Bamba, C. Q. Geng and C. C. Lee, J. Cosmol. Astropart. Phys. 08 (2010) 021, arXiv:1005.4574.

[32] A. A. Starobinsky, Adv. Ser. Astrophys. Cosmol. **3**, 130-133 (1987) doi:10.1016/0370-2693(80)90670-X K. Bamba, S. Nojiri, S. D. Odintsov and D. Sáez-Gómez, Phys. Rev. D **90**, 124061 (2014) doi:10.1103/PhysRevD.90.124061 [arXiv:1410.3993 [hep-th]].

[33] S. Nojiri and S. D. Odintsov, Gen. Rel. Grav. **38**, 1285-1304 (2006) doi:10.1007/s10714-006-0301-6 [arXiv:hep-th/0506212 [hep-th]]; S. Nojiri, S. D. Odintsov and D. Saez-Gomez, Phys. Lett. B **681**, 74-80 (2009) doi:10.1016/j.physletb.2009.09.045 [arXiv:0908.1269 [hep-th]].

[34] S. D. Odintsov, D. Saez-Chillon Gomez, G. S. Sharov, Eur. Phys. J. C 77 (2017) 862, arXiv:1709.06800.

[35] S. D. Odintsov, D. Saez-Chillon Gomez and G. S. Sharov, Phys. Rev. D. 99 (2019) 024003, arXiv:1807.02163.

[36] E. Elizalde, S. Nojiri, S.D. Odintsov, L. Sebastiani and S. Zerbini, Phys. Rev. D. 83 (2011) 086006, arXiv:1012.2280.

[37] S. Nojiri, S. D. Odintsov and V. K. Oikonomou, Phys. Dark Univ. 29 (2020) 100602, arXiv:1912.13128.

[38] S. D. Odintsov and V. K. Oikonomou, Phys. Rev. D. 99 (2019) 104070, arXiv:1905.03496.

[39] S. D. Odintsov and V. K. Oikonomou, Phys. Rev. D. 101 (2020) 044009, arXiv:2001.06830.

[40] G. Cognola, E. Elizalde, S. Nojiri, S. D. Odintsov, L. Sebastiani and S. Zerbini, Phys. Rev. D 77 (2008) 046009, arXiv:0712.4017.

[41] S. D. Odintsov, D. Saez-Chillon Gomez and G. S. Sharov, Phys. Rev. D. 101 (2020) 044010, arXiv:2001.07945.

[42] G. S. Sharov, J. Cosmol. Astropart. Phys. 06 (2016) 023, arXiv:1506.05246.

[43] S. Pan and G. S. Sharov, Mon. Not. Roy. Astron. Soc. 472 (2017) 4736, arXiv:1609.02287.

[44] G. S. Sharov and S. E. Sinyakov, Math. Modelling and Geometry 8 (2020) 1, arXiv:2002.03599.

[45] D. M. Scolnic et al., Astrophys. J. 859 (2018) 101, arXiv:1710.00845.

[46] L. Chen, Q.-G. Huang and K. Wang, J. Cosmol. Astropart. Phys. 1902 (2019) 028, arXiv:1808.05724.

[47] J. Simon, L. Verde and R. Jimenez, Phys. Rev. D 71 (2005) 123001, astro-ph/0412269; D. Stern, R. Jimenez, L. Verde, M. Kamionkowski and S. A. Stanford, JCAP 1002 (2010) 008, arXiv:0907.3149; M. Moresco et al., JCAP 1208 (2012) 006, arXiv:1201.3609; C. Zhang et al., Res. Astron. Astrophys. 14 (2014) 1221, arXiv:1207.4541; M. Moresco, Mon. Not. Roy. Astron. Soc. 450(1) (2015) L16, arXiv:1503.01116; M. Moresco et al., JCAP 1605 (2016) 014, arXiv:1601.01701; A. L. Ratsimbazafy et al. Mon. Not. Roy. Astron. Soc. 467(3) (2017) 3239, arXiv:1702.00418.

[48] E. Gaztañaga, A. Cabre and L. Hui, Mon. Not. Roy. Astron. Soc. 399 (2009) 1663, arXiv:0807.3551; C. Blake et al., Mon. Not. Roy. Astron. Soc. 425 (2012) 405, arXiv:1204.3674; C. H. Chuang and Y. Wang, Mon. Not. Roy. Astron. Soc. 435 (2013) 255, arXiv:1209.0210; C-H. Chuanget et al., Mon. Not. Roy. Astron. Soc. 433 (2013) 3559, arXiv:1303.4486;

N. G. Busca et al., *Baryon Acoustic Oscillations in the Lyα forest of BOSS quasars.* Astron. and Astrophys. 552 (2013) A96, arXiv:1211.2616; A. Oka et al., Mon. Not. Roy. Astron. Soc. 439 (2014) 2515, arXiv: 1310.2820; A. Font-Ribera et al., J. Cosmol. Astropart. Phys. 05 (2014) 027, arXiv:1311.1767; T. Delubac et al., Astron. Astrophys. 574 (2015) A59, arXiv:1404.1801; L. Anderson et al., Mon. Not. Roy. Astron. Soc. 441 (2014) 24 arXiv:1312.4877; Y. Wang et al., Mon. Not. Roy. Astron. Soc. 469 (2017) 3762, arXiv:1607.03154; S. Alam et al., Mon. Not. Roy. Astron. Soc. 470 (2017) 2617, arXiv:1607.03155; J. E. Bautista et al., Astron. Astrophys. 603 (2017) id. A12, arXiv:1702.00176.

[49] F. Zhu, N. Padmanabhan, A. J. Ross et al., Mon. Not. Roy. Astron. Soc. 480 (2018) 1096, arXiv:1801.03038; G.-B. Zhao, Y. Wang, S. Saito et al., Mon. Not. Roy. Astron. Soc. 482 (2019) 3497, arXiv:1801.03043.

[50] G. S. Sharov and V.O. Vasiliev, Math. Modelling and Geometry 6 (2018) 1, arXiv:1807.07323.

[51] H. Akaike, IEEE Transactions on Automatic Control, 19 (1974) 716.